

# BRAIN COMMUNICATIONS

## Regional associations of white matter hyperintensities and early cortical amyloid pathology

 Luigi Lorenzini,<sup>1</sup> Loes T. Ansems,<sup>1</sup> Isadora Lopes Alves,<sup>1</sup> Silvia Ingala,<sup>1</sup>  
 David Vázquez García,<sup>1</sup> Jori Tomassen,<sup>2</sup> Carole Sudre,<sup>3,4,5</sup> Gemma Salvadó,<sup>6,7</sup>  
Mahnaz Shekari,<sup>6,7,8</sup> Gregory Operto,<sup>6,7,9</sup> Anna Brugulat-Serrat,<sup>6,7,9,10</sup>  
Gonzalo Sánchez-Benavides,<sup>6,7,9</sup> Mara ten Kate,<sup>1,2</sup>  Betty Tijms,<sup>2</sup>  Alle Meije Wink,<sup>1</sup>  
Henk.J.M.M. Mutsaerts,<sup>1</sup> Anouk den Braber,<sup>2,11</sup> Pieter Jelle Visser,<sup>2,12</sup> Bart N.M. van  
Berckel,<sup>1</sup>  Juan Domingo Gispert,<sup>6,7,8,13</sup> Frederik Barkhof,<sup>1,14</sup>  Lyduine E. Collij,<sup>1</sup>  
On behalf of the AMYPAD consortium and On behalf of the EPAD consortium for the ALFA cohort

White matter hyperintensities (WMHs) have a heterogeneous aetiology, associated with both vascular risk factors and amyloidosis due to Alzheimer's disease. While spatial distribution of both amyloid and WM lesions carry important information for the underlying pathogenic mechanisms, the regional relationship between these two pathologies and their joint contribution to early cognitive deterioration remains largely unexplored.

We included 662 non-demented participants from three Amyloid Imaging to Prevent Alzheimer's disease (AMYPAD)-affiliated cohorts: EPAD-LCS (N = 176), ALFA+ (N = 310), and EMIF-AD PreclinAD Twin60++ (N = 176). Using PET imaging, cortical amyloid burden was assessed regionally within early accumulating regions (medial orbitofrontal, precuneus, and cuneus) and globally, using the Centiloid method. Regional WMH volume was computed using Bayesian Model Selection. Global associations between WMH, amyloid, and cardiovascular risk scores (Framingham and CAIDE) were assessed using linear models. Partial least square (PLS) regression was used to identify regional associations. Models were adjusted for age, sex, and *APOE-e4* status. Individual PLS scores were then related to cognitive performance in 4 domains (attention, memory, executive functioning, and language).

While no significant global association was found, the PLS model yielded two components of interest. In the first PLS component, a fronto-parietal WMH pattern was associated with medial orbitofrontal-precuneal amyloid, vascular risk, and age. Component 2 showed a posterior WMH pattern associated with precuneus-cuneus amyloid, less related to age or vascular risk. Component 1 was associated with lower performance in all cognitive domains, while component 2 only with worse memory.

In a large pre-dementia population, we observed two distinct patterns of regional associations between WMH and amyloid burden, and demonstrated their joint influence on cognitive processes. These two components could reflect the existence of vascular-dependent and -independent manifestations of WMH-amyloid regional association that might be related to distinct primary pathophysiology.

- 1 Dept. of Radiology and Nuclear Medicine, Amsterdam University Medical Center, Amsterdam Neuroscience, Amsterdam, The Netherlands
- 2 Department of Neurology, Alzheimer Center Amsterdam, Amsterdam Neuroscience, Vrije Universiteit Amsterdam, Amsterdam UMC, Amsterdam, The Netherlands
- 3 Centre for Medical Image Computing (CMIC), Departments of Medical Physics & Biomedical Engineering and Computer Science, University College London, UK
- 4 MRC Unit for Lifelong Health and Ageing - University College London, UK

Received March 24, 2022. Revised April 11, 2022. Accepted June 9, 2022. Advance access publication June 15, 2022

© The Author(s) 2022. Published by Oxford University Press on behalf of the Guarantors of Brain.

This is an Open Access article distributed under the terms of the Creative Commons Attribution License (<https://creativecommons.org/licenses/by/4.0/>), which permits unrestricted reuse, distribution, and reproduction in any medium, provided the original work is properly cited.

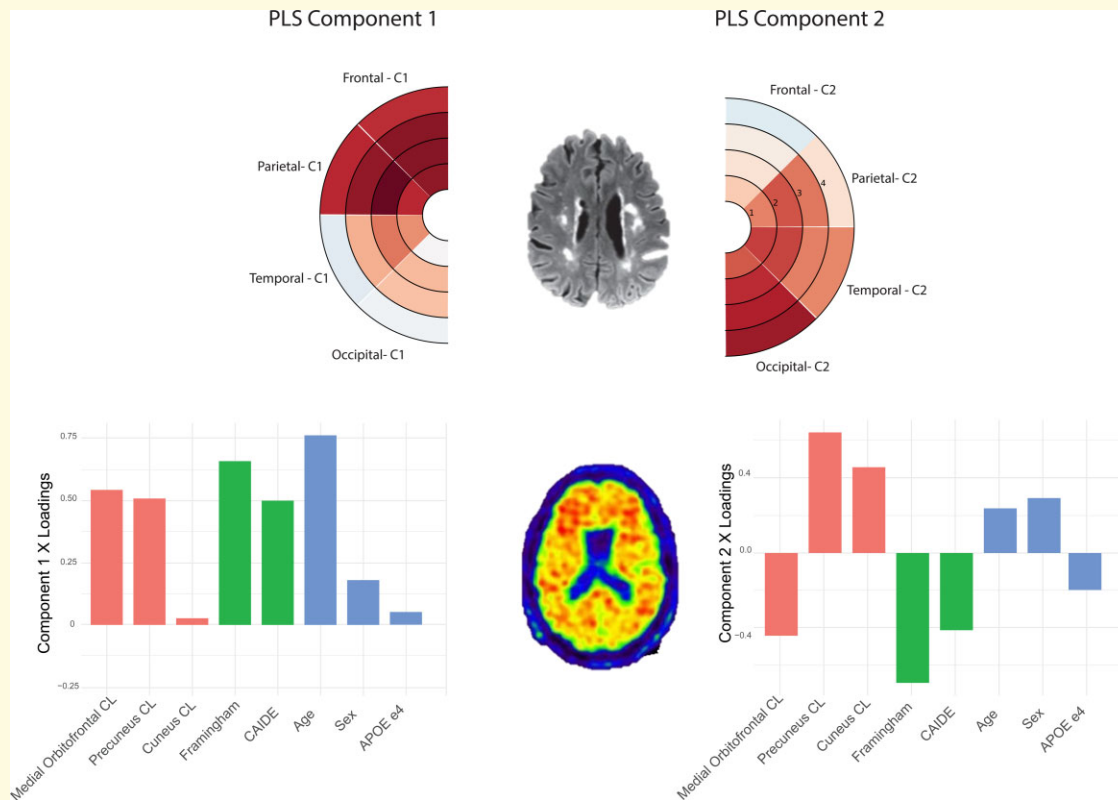
- 5 School of Biomedical Engineering, King's College London UK  
 6 BarcelonaBeta Brain Research Center (BBRC), Pasqual Maragall Foundation, Barcelona, Spain  
 7 IMIM (Hospital del Mar Medical Research Institute), Barcelona, Spain  
 8 Universitat Pompeu Fabra, Barcelona, Spain  
 9 Centro de Investigación Biomédica en Red de Fragilidad Y Envejecimiento Saludable (CIBERFES), Madrid, Spain  
 10 Atlantic Fellow for Equity in Brain Health at the University of California San Francisco, San Francisco, California, USA  
 11 Department of Biological Psychology, Vrije Universiteit Amsterdam, Neuroscience Amsterdam, Amsterdam, The Netherlands  
 12 Department of Psychiatry and Neuropsychology, School for Mental Health and Neuroscience, Maastricht University, Maastricht, The Netherlands  
 13 Centro de Investigación Biomédica en Red Bioingeniería, Biomateriales Y Nanomedicina, Madrid, Spain  
 14 Queen Square Institute of Neurology and Centre for Medical Image Computing, University College London, London, UK

Correspondence to: Luigi Lorenzini, MSc  
 Dep. of Radiology and Nuclear Medicine, PK -1  
 De Boelelaan 1117  
 1081 HV Amsterdam, The Netherlands  
 E-mail: l.lorenzini@amsterdamumc.nl

**Keywords:** white matter hyperintensities; amyloid PET; regional associations; multivariate analysis; pre-dementia population

**Abbreviations:** ALFA = Alzheimer and Families; AMYPAD = Amyloid Imaging to Prevent Alzheimer's disease; CAIDE = Cardiovascular Risk Factors, Aging, and Incidence of Dementia; CDR = Clinical Dementia Rating; CL = Centiloid; EOAD = early-onset Alzheimer's disease; EPAD-LCS = European Prevention of Alzheimer's Dementia Longitudinal Cohort Study; LOAD = late-onset Alzheimer's disease; MMSE = Mini-Mental State Examination; PLS = partial least square; ROI = region of interest; SVD = small-vessel disease; WMHs = white matter hyperintensities.

## Graphical Abstract



## Introduction

White matter hyperintensities (WMHs) and cortical amyloid deposition are imaging hallmarks of the two most common causes of dementia.<sup>1</sup> WMHs, as measured on T<sub>2</sub>-weighted MRI, are markers of small-vessel disease (SVD). They are prevalent in cognitively unimpaired older individuals and associated with vascular risk factors.<sup>2,3</sup> Amyloid- $\beta$  pathology (A $\beta$ ) is hypothesized to initiate the Alzheimer's disease pathological cascade,<sup>4,5</sup> followed by the aggregation of intraneuronal hyperphosphorylated tau (p-tau), and eventual grey matter volume loss.<sup>6,7</sup> Both WMH and amyloid burden can be observed years before the onset of cognitive symptoms and have been shown to contribute to cognitive impairment.<sup>8,9</sup>

Despite their diverse aetiologies, the frequent co-occurrence of WMH and cerebral amyloid suggests a possible interaction of these two pathologies.<sup>3</sup> For example, WMH-related impaired perivascular drainage has been shown to obstruct A $\beta$  clearance, thus facilitating aggregation of A $\beta$  proteins.<sup>10</sup> In turn, cerebral amyloidosis can induce vasoconstriction and vessel wall damage, thus resulting in WMH development independently of vascular risk factors.<sup>11</sup> Importantly, previous studies have underlined the spatial heterogeneity of WMH aetiology,<sup>12</sup> showing that while systemic vascular factors relate to increased frontal WMH, posterior lesions are observed in relationship to amyloid deposition.<sup>13,14</sup>

However, to date the spatial distribution of amyloid burden has not been taken into account, while several early accumulating regions have been identified.<sup>15</sup> Consequently, the correspondence and interaction of these two pathological image features has not been investigated on a regional level. Understanding the regional relationship between cerebral amyloid pathology and white matter damage, and its interplay with systemic vascular risk factors, is therefore important for an accurate characterization of the multifactorial processes leading to early cognitive impairment in neurodegenerative diseases.

In this work, we investigated the relationship between the regional distribution of WMH and amyloid burden in a large cohort of pre-dementia individuals from three parent cohorts involved in the Amyloid Imaging to Prevent Alzheimer's disease (AMYPAD) consortium.<sup>16</sup> To this aim, we first used linear analysis for the exploration of global association between WMH and amyloid. Then, we performed a multivariate partial least square (PLS) regression investigating the interplay between regional amyloid burden and systemic vascular risk factors in promoting differential patterns of WMH. Eventually, we assessed the joint contribution of these two pathologies to cognitive performance.

## Materials and methods

### Cohorts

Data were drawn from the ALFA+ cohort, European Medical Information Framework for Alzheimer's disease—

PreclinAD Twin60++ (hereafter PreclinAD), and European Prevention of Alzheimer's Dementia Longitudinal Cohort Study (EPAD-LCS). All cohorts are affiliated with the AMYPAD Prognostic and Natural History Study (PNHS).<sup>16</sup> The ALFA+ cohort is a nested longitudinal study of the ALFA (for Alzheimer's and Families) study to characterize preclinical Alzheimer's disease in cognitively unimpaired individuals who underwent amyloid PET imaging.<sup>17</sup> The protocols have been approved by an independent Ethics Committee Parc de Salut Mar Barcelona and registered at Clinicaltrials.gov (ALFA+ Identifier: NCT02685969). The PreclinAD cohort included monozygotic twins from the Amsterdam sub-study of the European Medical Information Framework and is a longitudinal study on risk factors for amyloid pathology and cognitive decline in cognitively normal older adults.<sup>18</sup> The study was approved by the VU University Medical Center's ethics committee. The EPAD-LCS cohort recruited participants across 21 European sites across the full range of anticipated probability for Alzheimer's disease development that aims at characterizing the preclinical and prodromal stages of Alzheimer's disease, by creating a pool of well characterized individuals for recruitment in potential pharmacological trials.<sup>19</sup> Institutional review boards of each participating centre approved the EPAD-LCS study.

### Participants

The ALFA+ cohort selected participants who were aged between 45 and 65 years enriched for family history of Alzheimer's disease or *APOE* $\epsilon$ 4 carriership and a global Clinical Dementia Rating (CDR) score of 0.<sup>17,20</sup> The PreclinAD cohort inclusion criteria were having age above 60 years, a delayed recall score of  $>-1.5$  SD of age-adjusted normative data on the Consortium to Establish a Registry for Alzheimer's Disease (CERAD) 10-word list,<sup>21</sup> a global CDR score of 0, Telephone Interview for Cognitive Status modified (TICS-m) score of 23 or higher,<sup>22</sup> and a 15-item Geriatric Depression Scale score of  $<11$ .<sup>23</sup> Eligibility criteria in the EPAD-LCS cohort were age above 50 years, CDR score of  $<1$ , and no known diagnosis of dementia.<sup>19</sup> For this study, we selected participants with PET and MRI  $<1$  year apart from each other. Demographics and clinical characteristics were available from all cohorts. Individuals *APOE* genotyping was re-coded as being either  $\epsilon$ 4 non-carriers,  $\epsilon$ 4 heterozygous or  $\epsilon$ 4 homozygous. Owing to *APOE*  $\epsilon$ 2/ $\epsilon$ 4 genotype indeterminate relationship with Alzheimer's disease and vascular risk factor, participants with this variant were excluded from the analysis. In total, 662 subjects were included in this study, of which 311 ALFA+, 176 PreclinAD and 175 EPAD-LCS subjects.

### Neuropsychological assessment

All participants underwent cognitive testing including the Mini-Mental State Examination (MMSE). Moreover, each cohort assessed cognitive domains using comprehensive

standardized neuropsychological test batteries. Attention, memory (average between delayed and immediate memory in the EPAD cohort) and language cognitive domain scores were available across all cohorts. Therefore, we pulled cognitive performance on these three domains between cohorts by Z-scoring within each cognitive domain and cohort. Executive functioning domain was only available in PreclinAD and ALFA+ cohort. Visuo-constructional domain was only available in the EPAD cohort. Specific test and domain composite score description for each cohort can be found in the [Supplementary Materials](#).

## Vascular risk scores

Individual vascular risk was computed by means of composite risk factor scores: the Cardiovascular Risk Factors, Aging, and Incidence of Dementia (CAIDE) and the Framingham Risk Score (FRS). The CAIDE score estimates the risk of developing late life dementia based on midlife vascular risk factors.<sup>24</sup> The original scoring system for CAIDE uses information on age, sex, education, high blood pressure (BP), body mass index (BMI), total cholesterol and physical inactivity. The FRS is a sex-specific algorithm used to estimate the 10-year cardiovascular risk of an individual. It uses information on age, sex, systolic BP, antihypertensive medication, diabetes, total and HDL cholesterol and smoking.<sup>25</sup> In the absence of blood biomarkers, self-reported hypercholesterolaemia was used to score cholesterol related information and re-coded as described in Calvin *et al.*<sup>26</sup> Both scores were computed with and without including age, to check for possible over-corrections in later analysis.

## PET acquisition and processing

Amyloid PET scans from the ALFA+ (Siemens Biograph mCT scanner) and the PreclinAD (Philips Ingenuity Time-of-Flight PET–MRI scanner) cohorts were obtained with four frames (4 × 5 min) acquired 90–110 min post-injection of [<sup>18</sup>F]flutemetamol.<sup>18,27</sup> Images were checked for motion and inter-frame registration was performed. Subsequently, the four frames from the PET images were averaged and registered to the corresponding 3D T<sub>1</sub>-weighted (T1w) MRI images. Then, the T1w images were registered to standard space and the same transformation was applied to the co-registered PET images, using SPM12.<sup>18,27</sup> For the EPAD-LCS cohort, PET acquisition was performed under the AMYPAD PNHS protocol and consisted of four frames (4 × 5 min), acquired 90–110 min post-injection of [<sup>18</sup>F]flutemetamol or [<sup>18</sup>F]florbetaben.<sup>16</sup> PET frames were averaged, co-registered to the corresponding MRI scans, and registered to the Montreal Neurological Institute space using SPM12.

PET images were intensity-normalized using the cerebellum as a reference region using the mask provided by the Centiloid (CL) project<sup>28</sup> (<http://www.gaain.org/centiloid-project>). In the CL scale, CL = 0 corresponds with absence of amyloid in young controls, and CL = 100 corresponds

with the burden of a typical mild-to-moderate Alzheimer's disease dementia patient.<sup>28</sup> Cortical Centiloid values were calculated using the standard target region and a previously calibrated conversion equation for ALFA+ and PreclinAD cohorts<sup>29</sup> and the calibrated conversion equations for [<sup>18</sup>F]flutemetamol and [<sup>18</sup>F]florbetaben for the EPAD-LCS cohort.

Three regions of interest (ROIs) were created from the Learning Embeddings for Atlas Propagation (LEAP)<sup>30</sup> atlas to capture amyloid pathology across early anterior and posterior regions:<sup>31</sup> medial orbitofrontal cortex (gyrus rectus and medial frontal cortex), precuneus and cuneus. Regional standard uptake value ratios were extracted from these three ROIs and converted to regional Centiloid units using the global conversion equation.<sup>28</sup>

## MRI acquisition and processing

In the ALFA+ cohort, scans were obtained with a 3 T scanner (Ingenia CX, Philips Healthcare, Best, The Netherlands). The MRI protocol included a 3D T1w Turbo Field Echo (TFE) sequence (voxel size 0.75 × 0.75 × 0.75 mm, TR/TE: 9.90/4.6 ms, flip angle = 8°) and a 3D T2-FLAIR sequence (TSE, voxel size 1 × 1 × 1 mm, TR/TE/TI: 5000/312/1700 ms). Scans were visually assessed for quality and incidental findings by a trained neuroradiologist.<sup>32</sup> In the PreclinAD cohort, MRI scans were obtained using a single 3 T scanner (Philips Ingenuity Time-of-Flight PET/MRI scanner) with a 8-channel head coil. The scan protocol included T1w sequences, acquired using sagittal turbo field echo sequence (1.00 mm<sup>3</sup> isotropic voxels, TR/TE = 7.9 ms/4.5 ms, and flip angle = 8°), and 3D sagittal FLAIR sequences (1.12 mm<sup>3</sup> isotropic voxels, TR/TE = 4800/279 ms, and inversion time = 1650 ms).<sup>33</sup> The EPAD-LCS baseline data were acquired at 21 different EPAD-LCS sites. The core MRI protocol was performed on all consented participants and included 3D T1w, 3D FLAIR, 2D T2w and 2D T2\* acquisition. Details on the MRI acquisition parameters and processing steps are previously described.<sup>34</sup>

WMH segmentation was performed using Bayesian Model Selection (BaMoS), an unsupervised model selection framework.<sup>35</sup> Regional values of WMH were obtained by averaging lesions within atlas regions taking into account lobar boundaries (frontal, parietal, temporal, and occipital) and distance between the ventricular surface and cortex (4 layers) and depicted using bullseye plot representation.<sup>36</sup> In this work, WMH regional values were averaged between the left and right hemisphere. Total intracranial volume was also calculated for normalization purposes, using a previously validated method.<sup>37</sup>

## Statistical analysis

All analyses were carried out in R version 4.0.3. Differences in demographics among the three cohorts were assessed using one-way ANOVA and Kruskal–Wallis tests for numerical and categorical variables, respectively. Data

normalization for statistical analysis was performed within each cohort ([Supplementary Materials](#)).

### Association between amyloid and global white matter hyperintensities burden

The cross-sectional association between global amyloid burden (independent variable) and normalized global WMH volumes (dependent variable) was assessed using linear models, with covariate adjustment by age, sex and *APOE* genotype. The same model was also run using each of the regional amyloid CL values and vascular risk scores as the main predictors.

### Regional relationship between amyloid and white matter hyperintensities burden

Considering the high cross-correlations within the WMH and amyloid data sets, we assessed their regional relationship using PLS regression. PLS models relationships between two multivariate data sets, by finding linear combinations of predictors (e.g. regional amyloid) that maximally explain the variance in the outcome variables (e.g. regional WMH), maximizing the covariance between the two data sets.<sup>38</sup> The contribution of each variable into each component is expressed as variable loadings, while PLS scores summarize individual observations, i.e. participants, into the estimated components.<sup>39</sup>

The PLS model was built in R using the *pls* package (version 2.7–3). Regional CL values, framingham and CAIDE vascular risk scores were included in the model as predictors. All the 16 regional WMH values were used as outcome measures. Age, sex, and *APOE* genotype were added to the predictors matrix as covariates. The best number of fitting latent components was determined using the cross-validation approach previously described.<sup>38</sup>

### Relationship of partial least square components with cognitive domains

We further evaluated the joint contribution of regional WMH, regional amyloid, and vascular risk scores to cognitive performance. Linear models were used to investigate the effects of component scores onto performance in cognitive domains. Attention, memory and language performance were studied across cohorts, visuo-constructional performance in the EPAD participants only and executive functioning in the PreclinAD and ALFA+ only.

## Data Availability

The data used in this manuscript are available upon request from the specific projects involved.

## Results

### Cohort characteristics

Demographics and clinical characteristics are shown in [Table 1](#). Mean age was 64.9 years ( $SD = 7.19$ ), and 261 (39%) were male. Participants were without dementia ( $CDR = 0$ :  $N = 613$ , 92.60%;  $CDR = 0.5$ :  $N = 49$ , 7.40%)

at inclusion with an average MMSE of 29.01 over the whole group. Higher global amyloid burden as expressed in CL units were observed in the EPAD participants compared with the other two cohorts. WMH load was lower in the ALFA+ cohort compared with EPAD and PreclinAD.

### Global white matter hyperintensities and cortical amyloid

Both global and regional amyloid burden did not show any significant effect on global values of WMH lesions. Vascular risk scores had a significant positive relationship with global WMH load, with high scores being related to greater WM lesions. Covariates coefficients showed significant influences of age on global WMH load, with older age being associated with more WM lesions ([Table 2](#)).

### Multivariate white matter hyperintensities and cortical amyloid relationship

Cross-validation identified two components as being the optimal number of components, i.e. yielding the lowest root mean square error in the PLS model explaining regional variability in WMH (see [Supplementary Materials](#)).

The first component (C1; [Fig. 1](#)) showed positive PLS loadings of frontal and parietal WMH, with highest values in the second and third, i.e. deep white matter layers. Temporal and occipital volumes of WMH demonstrated low contributions to this component. The contribution of the predictor variables, i.e. x loadings, showed that vascular risk scores had the highest PLS positive loadings to the C1 together with age. Medial orbitofrontal and precuneus amyloid measures were also positively related to this component, while cuneal amyloid showed no relationship.

In the second component (C2; [Fig. 1](#)), a posterior WMH regional pattern was found. A strong involvement of occipital WMH was observed for all layers with high positive PLS component loadings. Temporal and parietal WMH also showed mild positive contribution to C2 mostly in periventricular regions. Low PLS loadings were found for frontal WMH regions, with negative values in the 4th layer. This posterior pattern of WMH was mainly positively associated with precuneal and cuneal amyloid burden. Moreover, Framingham and CAIDE risk scores were negatively associated with C2. Compared to C1, this component was less related to age. All PLS loadings are reported in [Supplementary Table 1](#) and [Supplementary Table 2](#).

These results were highly consistent when correcting for cohort ([Supplementary Figs 3–6](#)).

### Relationship of partial least square components with cognitive domains

We further used individual participants' scores from the PLS model, i.e. the contribution of each observation to the components, to investigate their relationship with cognitive

**Table 1** Participants' characteristics. Demographic and clinical characteristics of included participants are reported stratifying per cohort

|                           | Whole population (n = 662) | ALFA (n = 311)    | EPAD (n = 175)    | PreclinAD (n = 176) |
|---------------------------|----------------------------|-------------------|-------------------|---------------------|
| Age (years)               | 64.90 (7.19)               | 61.11 (4.51)      | 66.29 (6.98)      | 70.22 (7.39)        |
| Sex = M (n; %)            | 261 (39.4)                 | 113 (36.3)        | 77 (44.0)         | 71 (40.3)           |
| Education (years)         | 14.18 (3.90)               | 13.43 (3.53)      | 14.57 (3.74)      | 15.11 (4.43)        |
| MMSE                      | 29.01 (1.23)               | 29.21 (0.95)      | 28.73 (1.63)      | 28.95 (1.16)        |
| CDR: 0.5 (%)              | 49 (7.40)                  | 0 (0)             | 49 (28)           | 0 (0)               |
| E4 carrier (n, %)         |                            |                   |                   |                     |
| Non-carrier               | 369 (55.7)                 | 143 (46.0)        | 105 (60.0)        | 121 (68.8)          |
| Heterozygote $\epsilon 4$ | 242 (36.6)                 | 136 (43.7)        | 57 (32.6)         | 49 (27.8)           |
| Homozygote $\epsilon 4$   | 51 (7.7)                   | 32 (10.3)         | 13 (7.4)          | 6 (3.4)             |
| Framingham Score          | 14.10 (4.01)               | 11.76 (2.83)      | 14.55 (4.00)      | 16.87 (3.46)        |
| CAIDE score               | 6.78 (2.08)                | 5.41 (1.48)       | 7.54 (1.91)       | 8.52 (1.36)         |
| Global Centiloid          | 12.32 (26.60)              | 2.73 (16.97)      | 26.92 (35.08)     | 14.76 (23.57)       |
| WMH total volume (mL)     | 4543.90 (6107.07)          | 3193.11 (3726.43) | 4798.18 (5930.91) | 6677.96 (8568.13)   |

MMSE = Mini-Mental State Examination; CDR = Clinical Dementia Rating score; CAIDE = Cardiovascular risk factors, aging and dementia; WMHs = White Matter Hyperintensities. Continuous variables are presented as mean (standard deviation), categorical variables as n (%).  $P < 0.001$

**Table 2** Association of global and regional amyloid, vascular risk scores and covariates with global WMH volume

|                      | Predictor                     | Estimate | Std. Error | P-value   |
|----------------------|-------------------------------|----------|------------|-----------|
| Amyloid              | Global CL                     | -0.009   | 0.014      | 0.51      |
|                      | Precuneus CL                  | -0.001   | 0.012      | 0.91      |
|                      | Medio-frontal CL              | -0.021   | 0.013      | 0.11      |
|                      | Cuneus CL                     | 0.001    | 0.023      | 0.98      |
| Vascular Risk Scores | Framingham Score              | 0.246    | 0.042      | <0.001*** |
|                      | CAIDE Score                   | 0.098    | 0.039      | <0.05*    |
| Covariates           | Age                           | 0.384    | 0.039      | <0.001*** |
|                      | Sex                           | -0.001   | 0.073      | 0.98      |
|                      | APOE                          | -0.076   | 0.079      | 0.33      |
|                      | $\epsilon 4$ -Heterozygous    |          |            |           |
|                      | APOE $\epsilon 4$ -Homozygous | 0.269    | 0.142      | 0.058     |

Results from linear models investigating the effect of candidate variables on global WMH. \*\*\* denotes a  $P$ -value < 0.001; \* denotes a  $P$ -value < 0.05. CL = Centiloid; CAIDE = Cardiovascular risk factors, aging and dementia.

performance. Higher scores in the C1 were related to worse performance in memory, attention and language across cohorts, and with the executive functioning domain in the ALFA+ and PreclinAD. C1 was not related to visuo-constructional domain (only investigated in the EPAD cohort). By contrast, C2 scores only showed a significant negative association with the memory domain across cohorts (Fig. 2). Within-cohorts association is reported in Supplementary Fig. 7.

## Discussion

In this large multi-cohort study of pre-dementia participants, we found two spatial patterns of WMH associated with

distinct profiles of regional cortical amyloid burden and vascular risk factors. First, fronto-parietal WMH load was related to amyloid burden in medial orbitofrontal and precuneus regions, with older age, and vascular risk factors. This component was related to cognitive functioning across all domains. Second, posterior WMH, mainly in occipital regions, was only positively associated with precuneus-cuneus amyloid. Higher scores of this component were related to worse memory functioning. These results suggest that the anterior and posterior WMH distributions are associated with different pathophysiologies, and advocate for a synergic contribution in promoting cognitive alterations typical of initial phases of neurodegenerative diseases.

Previous studies investigating the association of global WMH volume and amyloid burden have reported conflicting results.<sup>40</sup> While there is some evidence of a positive relation across the Alzheimer's disease spectrum,<sup>41</sup> other studies and the current one identified no significant global association between these two pathologies on a whole brain level.<sup>42</sup> However, the limited sensitivity of global scores to focal changes might have masked any regional associations between these two common pathologies. Using a multivariate statistical methodology, we provide further evidence for the existence of two interlinked regional patterns of WM lesions and amyloid deposition, highlighting the value of regional information for the understanding of the early interplay between these two pathologies.

In the first component, fronto-parietal lesions in the WM were positively related to medial orbitofrontal and precuneus amyloid burden, but also to vascular risk and age. In line with these results, recent neuropathological studies have observed frontal WMH in relationship to both SVD and amyloid-related degeneration.<sup>13</sup> Neuroimaging findings have also reported a more vascular involvement in the pathogenesis of frontal WM lesions,<sup>12</sup> putatively due the vulnerability of anterior and middle cerebral arteries to the development of SVD.<sup>43</sup> Moreover, WMH lesions at baseline have been associated specifically to amyloid accumulation over time in frontal

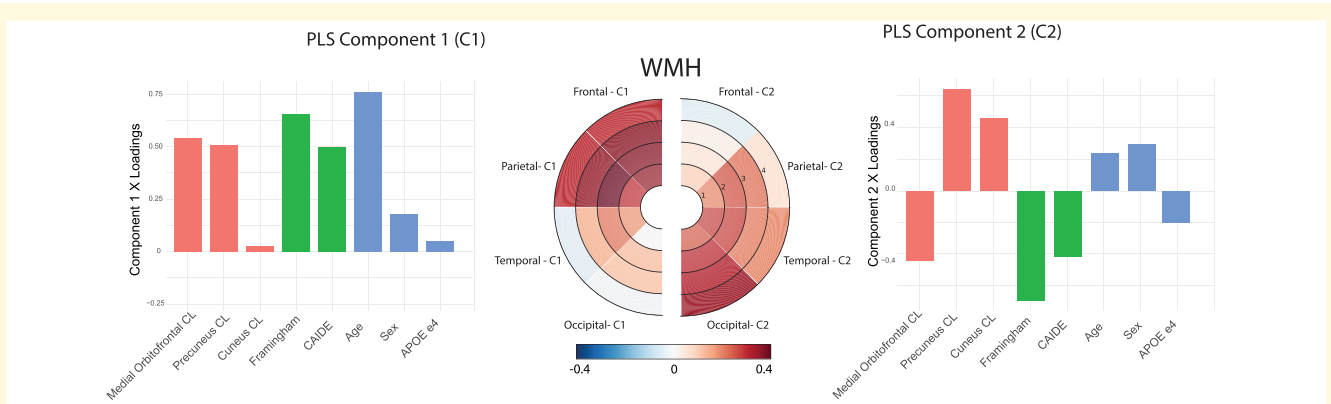


**Figure 1** Association of amyloid and vascular risk scores with regional WMHs volumes. Results of the PLS regression analysis on 662 participants. *Left:* Loadings of the used variables into the first PLS component (C1). *Right:* Loadings of the used variables into the second PLS component (C2). WMH loadings ( $y$  loadings) are reported using bullseye plots representing lobes and layers as described in a study by Sudre *et al.*<sup>36</sup> Loadings of regional amyloid (red, bar 1-3), vascular risk scores (green, bar 4-5) and covariates (blue, bar 6-8) are reported in a barplot ( $x$  loadings).

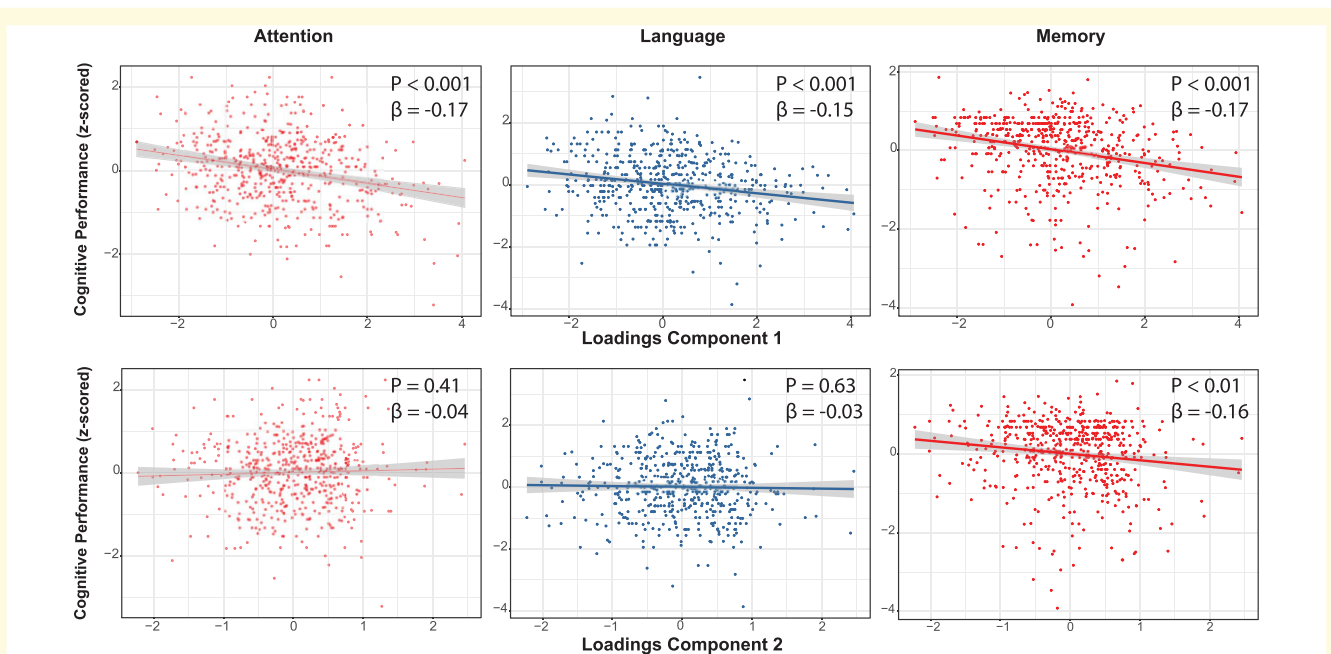


**Figure 2** Association of PLS regression components with cognitive performance. Upper row: Component 1 (C1) scores' relationship with attention (left), language (middle) and memory (right) performance across cohorts. Bottom row: Component 2 (C2) scores' relationship with attention (left), language (middle) and memory (right) performance across cohorts.  $P$ -values ( $P$ ) and beta coefficients ( $\beta$ ) are reported.

and parietal regions.<sup>44</sup> This vascular-related WMH and amyloid pattern in the fronto-parietal lobes is consistent with a line of recent research suggesting a strong contribution of cerebrovascular dysfunction in the development of dementia due to Alzheimer's disease.<sup>45</sup> Specifically, the *two-hits* framework proposes cerebrovascular damage to be an early insult sufficient to initiate neuronal injury and neurodegeneration by itself, but that can also influence the amyloidogenic pathway to diminish  $A\beta$  clearance and increase  $A\beta$  production, leading to elevated amyloid levels in the brain.<sup>46</sup> Considering the positive association of this component with older age, the proposed mechanism might be typical of the late-onset Alzheimer's disease (LOAD) symptomatology.<sup>47</sup> In fact, previous works have

shown that vascular dysregulation would indeed be an early event in the pathogenesis of LOAD, further confirming the possible role of cerebrovascular dysfunction in initiating this pathological cascade.<sup>48</sup> This component might therefore furnish neuroimaging evidence of the interplay between vascular and amyloid-related processes in the development of Alzheimer's disease and stress the importance of considering individualized vasculo-protective approaches for early treatment. However, the lack of longitudinal imaging data does not allow for a causal interpretation of this process. Further studies are therefore needed to exemplify the temporal relationship between vascular factors and anterior WMH and amyloid.





21. Moms JC, Heyman A, Mohs RC, et al. The Consortium to Establish a Registry for Alzheimer's Disease (CERAD). Part I. clinical and neuropsychological assesment of Alzheimer's disease. *Neurology*. 1989;39:1159–1159.
22. de Jager CA, Budge MM, Clarke R. Utility of TICS-M for the assessment of cognitive function in older adults. *Int J Geriatr Psychiatry*. 2003;18:318–324.
23. Yesavage JA, Brink TL, Rose TL, et al. Development and validation of a geriatric depression screening scale: A preliminary report. *J Psychiatr Res*. 1982;17:37–49.
24. Kivipelto M, Ngandu T, Laatikainen T, et al. Risk score for the prediction of dementia risk in 20 years among middle aged people: A longitudinal, population-based study. *Lancet Neurol*. 2006;5:735–741.
25. D'Agostino RB Sr, Vasan RS, Pencina MJ, et al. General cardiovascular risk profile for use in primary care: The Framingham Heart Study. *Circulation*. 2008;117:743–753.
26. Calvin CM, de Boer C, Raymont V, et al. Prediction of Alzheimer's disease biomarker status defined by the 'ATN framework' among cognitively healthy individuals: Results from the EPAD longitudinal cohort study. *Alzheimers Res Ther*. 2020;12.
27. Collij LE, Salvadó G, Shekari M, et al. Visual assessment of [18F]flutemetamol PET images can detect early amyloid pathology and grade its extent. *Eur J Nucl Med Mol Imaging*. 2021;48:2169–2182.
28. Klunk WE, Koeppe RA, Price JC, et al. The Centiloid Project: Standardizing quantitative amyloid plaque estimation by PET. *Alzheimers Dement*. 2015;11:1–15.e1–4.
29. Salvadó G, Molinuevo JL, Brugarat-Serrat A, et al. Centiloid cut-off values for optimal agreement between PET and CSF core AD biomarkers. *Alzheimers Res Ther*. 2019;11:27.
30. Wolz R, Aljabar P, Hajnal JV, et al. LEAP: Learning embeddings for atlas propagation. *Neuroimage*. 2010;49:1316–1325.
31. Collij LE, Ingala S, Altomare D, et al. Multitracer model for staging cortical amyloid deposition using PET imaging. *Neurology*. 2020;95:e1538–e1553.
32. Salvadó G, Brugarat-Serrat A, Sudre CH, et al. Spatial patterns of white matter hyperintensities associated with Alzheimer's disease risk factors in a cognitively healthy middle-aged cohort. *Alzheimers Res Ther*. 2019;vol. 11.
33. Ten Kate M, Sudre CH, den Braber A, et al. White matter hyperintensities and vascular risk factors in monozygotic twins. *Neurobiol Aging*. 2018;66:40–48.
34. Lorenzini L, Ingala S, Wink AM, Kuijter J, Wotschel V. The European Prevention of Alzheimer's Dementia (EPAD) MRI dataset and processing workflow. *bioRxiv*. 2021.
35. Sudre CH, Cardoso MJ, Bouvy WH, et al. Bayesian model selection for pathological neuroimaging data applied to white matter lesion segmentation. *IEEE Trans Med Imaging*. 2015;34:2079–2102.
36. Sudre CH, Gomez Anson B, Davagnanam I, et al. Bullseye's representation of cerebral white matter hyperintensities. *J. Neuroradiol*. 2018;45:114–122.
37. Cardoso MJ, Modat M, Wolz R, et al. Geodesic information flows: Spatially-variant graphs and their application to segmentation and fusion. *IEEE Trans Med Imaging*. 2015;34:1976–1988.
38. Boulesteix A-L, Strimmer K. Partial least squares: A versatile tool for the analysis of high-dimensional genomic data. *Brief Bioinform*. 2007;8:32–44.
39. Kvalheim OM, Karstang TV. Interpretation of latent-variable regression models. *Chemometrics Intellig Lab Syst*. 1989;7:39–51.
40. Roseborough A, Ramirez J, Black SE, Edwards JD. Associations between amyloid  $\beta$  and white matter hyperintensities: A systematic review. *Alzheimers Dement*. 2017;13:1154–1167.
41. Zhou Y, Zeidman P, Wu S, et al. Altered intrinsic and extrinsic connectivity in schizophrenia. *Neuroimage Clin*. 2018;17:704–716.
42. Vemuri P, Lesnick TG, Przybelski SA, et al. Vascular and amyloid pathologies are independent predictors of cognitive decline in normal elderly. *Brain*. 2015;138:761–771.
43. Shindo A, Ishikawa H, Ii Y, Niwa A, Tomimoto H. Clinical features and experimental models of cerebral small vessel disease. *Front Aging Neurosci*. 2020;12:109.
44. Moscoso A, Rey-Bretal D, Silva-Rodríguez J, et al. White matter hyperintensities are associated with subthreshold amyloid accumulation. *Neuroimage*. 2020;218:116944.
45. Soto-Rojas LO, Pacheco-Herrero M, Martínez-Gómez PA, et al. The neurovascular unit dysfunction in Alzheimer's disease. *Int J Mol Sci*. 2021;22.
46. Nelson AR, Sweeney MD, Sagare AP, Zlokovic BV. Neurovascular dysfunction and neurodegeneration in dementia and Alzheimer's disease. *Biochim Biophys Acta*. 2016;1862:887–900.
47. Rabinovici GD. Late-onset Alzheimer disease. *Continuum*. 2019;25:14–33.
48. Iturria-Medina Y, Sotero RC, Toussaint PJ, et al. Early role of vascular dysregulation on late-onset Alzheimer's disease based on multifactorial data-driven analysis. *Nat Commun*. 2016;7:11934.
49. Brickman AM, Provenzano FA, Muraskin J, et al. Regional white matter hyperintensity volume, not hippocampal atrophy, predicts incident Alzheimer disease in the community. *Arch Neurol*. 2012;69:1621–1627.
50. Duan J-H, Wang H-Q, Xu J, et al. White matter damage of patients with Alzheimer's disease correlated with the decreased cognitive function. *Surg Radiol Anat*. 2006;28:150–156.
51. Huang J, Friedland RP, Auchus AP. Diffusion tensor imaging of normal-appearing white matter in mild cognitive impairment and early Alzheimer disease: Preliminary evidence of axonal degeneration in the temporal lobe. *AJNR Am J Neuroradiol*. 2007;28:1943–1948.
52. Chen Y, Sillaire AR, Dallongeville J, et al. Low prevalence and clinical effect of vascular risk factors in early-onset Alzheimer's disease. *J Alzheimers Dis*. 2017;60:1045–1054.
53. Ossenkoppele R, Zwan MD, Tolboom N, et al. Amyloid burden and metabolic function in early-onset Alzheimer's disease: Parietal lobe involvement. *Brain*. 2012;135:2115–2125.
54. Hwang J, Kim CM, Kim JE, et al. Clinical Implications of Amyloid-Beta Accumulation in Occipital Lobes in Alzheimer's Continuum. *Brain Sci*. 2021;11.
55. Murman DL. The impact of age on cognition. *Semin Hear*. 2015;36:111–121.
56. Lampe J-H, Kharabian-Masouleh S, Kynast J, et al. Lesion location matters: The relationships between white matter hyperintensities on cognition in the healthy elderly. *J Cereb Blood Flow Metab*. 2019;39:36–43.
57. Lim YY, Maruff P, Pietrzak RH, et al. Effect of amyloid on memory and non-memory decline from preclinical to clinical Alzheimer's disease. *Brain*. 2014;137:221–231.
58. Lehmann M, Madison CM, Ghosh PM, et al. Intrinsic connectivity networks in healthy subjects explain clinical variability in Alzheimer's disease. *Proc Natl Acad Sci U S A*. 2013;110:11606–11611.
59. Thanprasertsuk S, Martinez-Ramirez S, Pontes-Neto OM, et al. Posterior white matter disease distribution as a predictor of amyloid angiopathy. *Neurology*. 2014;83:794–800.
60. Zhu Y-C, Chabriat H, Godin O, et al. Distribution of white matter hyperintensity in cerebral hemorrhage and healthy aging. *J Neurol*. 2012;259:530–536.